Journal of Computational Methods in Molecular Design, 2014, 4 (1):33-47

Scholars Research Library
(http://scholarsresearchlibrary.com/archive.html)

ISSN : 2231- 3176
CODEN (USA): JCMMDA

Quantum-chemical study of the relationships between electronic structure and anti- influenza activity. 1. The inhibition of cytopathic effects produced by the influenza A/Guangdong Luohu/219/2006 (H1N1) strain in MDCK cells by substituted acylamidobenzamides

Diego Muñoz-Gacitúa and Juan S. Gómez-Jeria*

Quantum Pharmacology Unit, Department of Chemistry, Faculty of Sciences, University of Chile. Las Palmeras 3425, Santiago 7800003, Chile

---

ABSTRACT

A quantum-chemical study of the relationships between electronic structure and the inhibition of cytophatic effects produced by the influenza A/Guangdong Luohu/219/2006 (H1N1) strain in MDCK cells by substituted acylamidobenzamides was carried out. The electronic structure of all the molecules was calculated within the Density Functional Theory at the B3LYP/6-31g(d,p) level with full geometry optimization. The cytotoxic activity of these molecules on this cell line was also analyzed. Despite the almost total lack of information regarding the mechanisms of antiviral action and cytotoxicity, we obtained statistically significant relationships between electronic structure and antiviral and cytotoxic activities. The variation of the antiviral activity is mainly orbital-controlled. The variation of cytotoxicity is charge- and orbital-controlled. The common skeleton used for his study seems to be correct. A short analysis of the MO-MO interaction is done. We suggest that the local atomic density of states, occupied and vacant, can be used as an approximate measure of the MO-MO penetration for the analysis of π-π stacking interactions.

Keywords: Influenza A, quantum pharmacology, quantitative structure-activity relationships, antiviral activity, H1N1 virus, substituted acylamidobenzamides, A/Guangdong Luohu/219/2006 (H1N1) strain.

INTRODUCTION

The influenza viruses are members of the *Orthomyxoviridae* family and are classified into three types, A, B and C, based on the antigenic differences in the nucleoprotein and matrix protein. Influenza A viruses can be additionally classified according to the serological reactivities of their antigenic surface proteins, hemagglutinin (HA) and neuraminidase (NA). There are 18 HA subtypes (H1-H18) and 11 NA (N1-N11) subtypes of influenza A virus that infect both avian and mammalian species [1-13]. Influenza A viruses are present in the avian reservoir [14-16]. In the twentieth century, three influenza viruses appeared in humans and caused major pandemics: the 1918 Spanish flu virus (H1N1, which infected 500 million of humans and caused the death of about 50-100 million people worldwide), the 1957 Asian flu virus (H2N2, which caused 1 million deaths) [17], and the 1968 Hong Kong flu virus (H3N2, with one million deaths in the 1969-1970 period). In April 2009, a new influenza A (H1N1) virus emerged among humans in California and Mexico, quickly spreading worldwide through human-to-human transmission, and generating the first influenza pandemic of the 21st century (18,000 deaths) [18]. The virus was found to be genetically related to viruses known to circulate in pigs. Interspecies transmission of influenza A viruses between humans and pigs is not infrequent and is reflected in the similarities of the subtypes H1N1 and H3N2 which have circulated in both species [19], and in the idea that pigs may act as an intermediate host in the appearance of novel human subtypes [6, 20, 21]. A new H7N9 influenza A virus first detected in March 2013 has caused more than

130 human infections in China, resulting in 40 deaths [22, 23]. It has been hypothesized that this new virus is a reassortant virus containing gene segments derived from four separate avian influenza viruses, including two different wild-bird viruses contributing the H7 hemagglutinin and N9 neuraminidase gene segments, and two different domestic poultry–derived H9N2 viruses contributing the other six internal genes [24, 25]. Thus, the search for novel synthetic and natural inhibitors that can circumvent these mutations remains essential [13, 26-41]. It is of importance then to produce the most reliable information possible coming from other fields of research, about the physical mechanism(s) underlying viral inhibition and any other important biological activities. To date there are no formal quantitative structure-activity relationship (QSAR) studies of families of antiviral molecules (for different approaches see [42, 43]. Here we present the results of a quantum-chemical analysis of the inhibitory activity of substituted acylamidobenzamides against the cytopathic effects produced by the influenza A/Guangdong Luohu/219/2006 (H1N1) strain in MDCK cells. The cytotoxic activity of these molecules on this cell line is also analyzed.

MATERIALS AND METHODS

The method.

Given that the model-based method [44] relating drug-receptor equilibrium constants with molecular structure has been described in great detail elsewhere [45-54], we present here only the final results in a standard formulation used before. The drug-receptor affinity constant, *log(K$_i$)* (or $log(IC_{50})$), is a linear function of several local atomic reactivity indices (LARIs) and has the following general form:

$$\log \mathrm{K}_i = a + bM_{D_i} + c\log\left[\sigma_{D_i} / (ABC)^{1/2}\right] + \sum_j \left[e_j Q_j + f_j S_j^E + s_j S_j^N\right] +$$
$$+ \sum_j \sum_m \left[h_j(m) F_j(m) + x_j(m) S_j^E(m)\right] + + \sum_j \sum_{m'} \left[r_j(m') F_j(m') + t_j(m') S_j^N(m')\right] +$$
$$+ \sum_j \left[g_j \mu_j + k_j \eta_j + o_j \omega_j + z_j \varsigma_j + w_j Q_j^{\max}\right] \quad (1)$$

where M is the drug molecule's mass, σ its symmetry number and ABC the product of the molecule's moment of inertia about the three principal axes of rotation. Q_i is the net charge of atom j, S_j^E and S_j^N are, respectively, the total atomic electrophilic and nucleophilic superdelocalizabilities of Fukui et al., $F_{j,m}$ ($F_{j,m'}$) is the Fukui index of the occupied (empty) MO m (m') located on atom j. $S_j^E(m)$ is the atomic electrophilic superdelocalizability of MO m on atom j, etc. [55]. The total atomic electrophilic superdelocalizability of atom j is the sum over occupied MOs of the $S_j^E(m)$'s and the total atomic nucleophilic superdelocalizability of atom j is the sum over empty MOs of the $S_j^N(m)$'s. The last bracket of the right side of Eq. 1 contains new local atomic reactivity indices obtained directly from LCAO-MO Theory by an approximate reorganization of part of the remaining terms of the series expansion used in the model [50]. μ_j is the local atomic electronic chemical potential of atom j (the HOMO$_j$*-LUMO$_j$* midpoint), η_j is the local atomic hardness of atom j (the HOMO$_j$*-LUMO$_j$* gap), ω_j is the local atomic electrophilicity of atom j (includes the predisposition of the electrophilic atom j to receive extra electronic charge together with its resistance to exchange charge with the medium), ς_j is the local atomic softness of atom j (the inverse of η_j) and $Q_j^{\max}$ is the maximal amount of electronic charge that atom j can accept from another site. HOMO$_j$* refers to the highest occupied molecular orbital localized on atom j and LUMO$_j$* to the lowest empty MO localized on atom j. They are called the local atomic frontier MOs. The molecule's MOs do not carry an asterisk.

The moment of inertia term can be expressed as:

$$\log\left[(ABC)^{-1/2}\right] = \sum_t \sum_t m_{i,t} R_{i,t}^2 = \sum_t O_t \quad (2)$$

where the summation over t is over the various substituents of the molecule, $m_{i,t}$ is the mass of the i-th atom belonging to the t-th substituent, $R_{i,t}$ being its distance to the atom to which the substituent is bonded. We proposed that the appearance of any O_t in a QSAR equation is related to its influence on the fraction of molecules attaining the correct orientation to interact with the receptor. We called the O_t's Orientational Parameters [56, 57]. The application of this method to the drug-receptor interaction has been very successful [47, 53, 54, 56, 58-66], and we have even been able to predict the *in vivo* activity of a hallucinogen [67-69] and to propose a cannabinoid derivative with enhanced receptor affinity [65].

Making use of additional hypothesis, we have proposed that $log(K_i)$ can be replaced by *log(BA)*, where *BA* is any biological activity measured *in vivo* or *in vitro* [70]. This extension was successfully applied to the uptake of some polychlorinated pollutant compounds by zucchini subspecies [71], the inhibition of virus-induced cytopathic effects by HIV and A-H1N1 virus [48], HIV-1 replication inhibition [70], antiproliferative activity against normal human fibroblasts and four human cancer cell lines [70], inhibitory strength toward hepatitis C virus (HCV) NS5B polymerase and inhibition of HCV replicons [51, 72].

Selection of the experimental data.

The selected molecules are a group of substituted acylamidobenzamides with antiviral activity against the influenza A/Guangdong Luohu/219/2006 (H1N1) strain [35]. The antiviral activity was evaluated as the inhibition of cytopathic effects (CPE) using MDCK (Madin-Darby canine kidney) cells with results reported as IC_{50}. The cytotoxicity of these compounds was evaluated in MDCK cells by the CPE method, with results reported as the median toxic concentrations, TC_{50}. The selected molecules are shown in Figure 1 and Table 1. It is important to notice that the antiviral action mechanism is uncertain. Ref. 34 states that viral hemagglutinin, neuraminidase and M2 protein can be ruled out as targets.

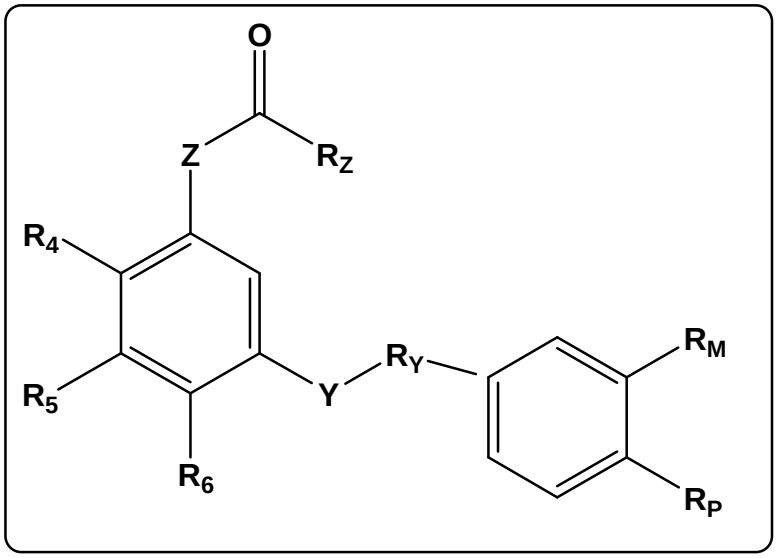

Figure 1. Substituted acylamidobenzamides.

Table 1. Acylamidobenzamides and their antiviral and cytotoxic activities.

Mol.	Z	Rz	Y	Ry	R4	R5	R6	Rm	Rp	log(TC_{50})	log(IC_{50}) H1N1
1	NH	C_2H_5	CO	NH	OCH_3	H	H	H	CH_3	2.21	1.37
2	NH	C_2H_5	CO	NH	OCH_3	H	H	H	Br	1.96	-
3	NH	C_2H_5	CO	NH	OCH_3	H	H	Cl	H	2.78	-
4	NH	C_2H_5	CO	NH	OCH_3	H	H	SCH_3	H	2.37	-
5	NH	$CH(Cl)CH_3$	CO	NH	OCH_3	H	H	H	H	2.30	1.24
6	NH	CH_3	CO	NH	OCH_3	H	H	H	H	--	2.05
7	NH	C_6H_5	CO	NH	OCH_3	H	H	H	H	2.28	1.10
8	NH	C_2H_5	CO	O	OCH_3	H	H	H	H	2.67	2.35
9	NH	C_2H_5	CO	NH	Cl	H	H	H	H	2.72	2.18
10	O	C_2H_5	CO	NH	OCH_3	H	H	H	H	2.71	2.24
11	NH	$CH(F)CH_3$	CO	NH	OCH_3	H	H	H	H	--	2.32
12	NH	$CH(F)CH_3$	CO	NH	H	OCH_3	H	H	H	2.69	2.32
13	NH	$CH(F)CH_3$	CO	NH	H	H	OCH_3	H	H	2.43	-
14	NH	$CH(F)CH_3$	CO	NH	H	H	H	H	H	2.76	2.16
15	NH	C_2H_5	CO	NH	OCH_3	H	H	H	NO_2	2.49	1.42
16	NH	C_2H_5	CO	NH	OCH_3	H	H	H	H	--	2.35
17	NH	C_2H_5	CO	$N(CH_3)$	OCH_3	H	H	H	H	2.65	2.00
18	NH	$CH(CH_3)_2$	CO	$N(CH_3)$	OCH_3	H	H	H	H	2.69	2.07
19	NH	C_2H_5	SO_2	NH	OCH_3	H	H	H	H	--	1.68
20	NH	C2H5	CO	NH	OCH3	H	H	H	H	--	1.6

Calculations.

The electronic structures of all the molecules were calculated within Density Functional Theory (DFT) at the B3LYP/6-31g(d,p) level with full geometry optimization. The Gaussian suite was used [73]. All the information needed to calculate numerical values for the local atomic reactivity indices was obtained from the Gaussian results with software written in our Unit. All electron populations smaller than or equal to 0.01 e were considered as zero. Negative electron populations coming from Mulliken Population Analysis were corrected as usual [74]. Molecular orbitals and molecular electrostatic potentials (MEP) were depicted using GaussView. Orientational parameters were calculated as usual [57]. Since the resolution of the system of linear equations is not possible because we did not have enough molecules, we made use of Linear Multiple Regression Analysis (LMRA) techniques to find the best solution. For each case, a matrix was built containing the dependent variable (the biological activity of each case) and the local atomic reactivity indices of all atoms of the common skeleton as independent variables (see Refs. [49, 54] for more details about the building of data matrices). The Statistica software was used for LMRA [75]. We worked within the *common skeleton hypothesis* stating that there is a definite collection of atoms, common to all molecules analyzed, that accounts for almost all the biological activity. The action of the substituents consists in modifying the electronic structure of the common skeleton and affecting the alignment of the drug through the orientational parameters. It is hypothesized that different parts or this entire common skeleton account for all the interactions leading to the expression of a given biological activity. The common skeleton for acylamidobenzamides is shown in Fig. 2.

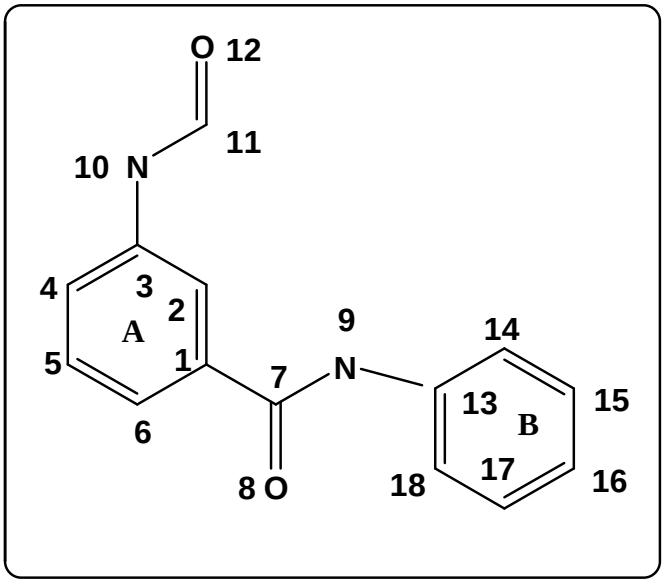

Figure 2. Numbering of atoms for the common skeleton of acylamidobenzamides used in this LMRA.

RESULTS

Results for the antiviral activity against the influenza A/Guangdong Luohu/219/2006 (H1N1) strain.

The statistically most significant equation obtained is:

$$log(IC_{50}) = 4.11 - 0.56s_{17} - 3.59S_7^E(HOMO-2)^* + 2.80F_4(LUMO+2)^* + 0.62F_{16}(LUMO+2)^* + 0.87S_{11}^E(HOMO-1)^* \quad (3)$$

with n=16, R=0.97, R^2=0.95, adj R^2=0.92, F(5,10)=37.59 (p<0.000001), outliers>2σ=0 and SD=0.12. s_{17} is the local atomic softness of atom 17 (see Fig. 2). $S_7^E(HOMO-2)^*$ and $S_{11}^E(HOMO-1)^*$ are, respectively, the local atomic superdelocalizability of the third local highest occupied MO of atom 7 and the local atomic superdelocalizability of the second local highest occupied MO of atom 11. $F_4(LUMO+2)^*$ and $F_{16}(LUMO+2)^*$ are, respectively, the Fukui indices (electron populations) of the third local lowest empty MOs of atoms 4 and 16. The beta coefficients and *t*-test for the significance of coefficients of Eq. 3 are shown in Table 2. Concerning independent variables, Table 3 shows that there are no significant internal correlations. The associated statistical parameters of Eq. 3 show that this equation is statistically significant and that the variation of a group of local atomic reactivity indices belonging to the common skeleton explains about 92% of the variation of the antiviral

activity against the influenza A/Guangdong Luohu/219/2006 (H1N1) strain. Figure 3 shows the plot of observed values *vs.* calculated ones.

Table 2. Beta coefficients and t-test for the significance of coefficients in Eq. 3.

Variable	Beta	B	t(10)	p-level
s_{17}	-0.89	-0.56	-11.39	<0.0000001
$S_7^E(HOMO-2)*$	-0.65	-3.56	-7.16	<0.00003
$F_4(LUMO+2)*$	0.45	2.80	5.26	<0.0004
$F_{16}(LUMO+2)*$	0.27	0.62	3.59	<0.005
$S_{11}^E(HOMO-1)*$	0.24	0.87	2.85	<0.02

Table 3. Squared correlation coefficients for the variables appearing in Eq. 3.

	s_{17}	$S_7^E(HOMO-2)*$	$F_4(LUMO+2)*$	$F_{16}(LUMO+2)*$
$S_7^E(HOMO-2)*$	0.10	1.00		
$F_4(LUMO+2)*$	0.001	0.24	1.00	
$F_{16}(LUMO+2)*$	0.07	0.07	0.04	1.00
$S_{11}^E(HOMO-1)*$	0.05	0.21	0.14	0.04

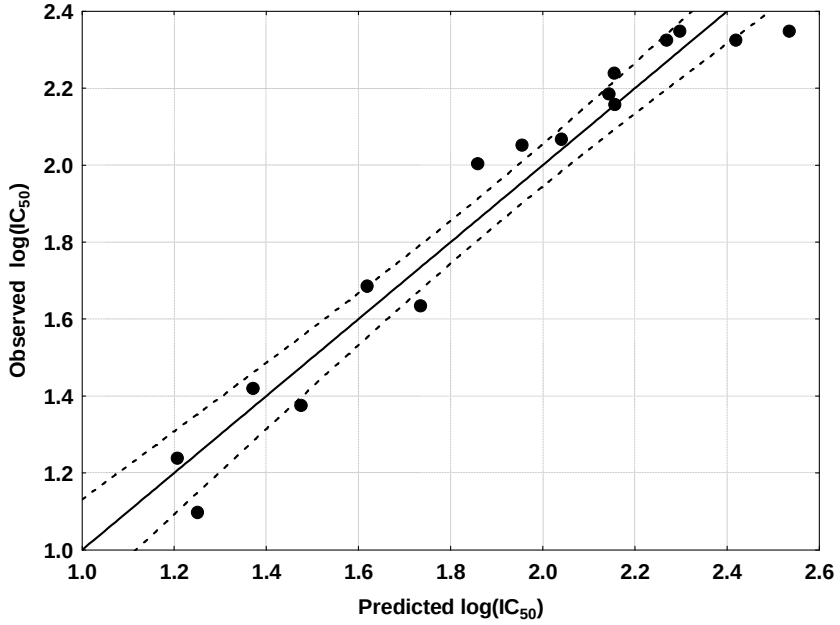

Figure 3. Plot of predicted *vs.* observed log(IC_{50}) values from Eq. 3. Dashed lines denote the 95% confidence interval.

Results for the cytotoxicity in MDCK cells.

The statistically most significant equation obtained is:

$$\log(TC_{50}) = 4.81 - 0.02S_9^N + 0.74F_{17}(LUMO)* + 3.27Q_{10} - 0.54F_2(HOMO-1)* \quad (4)$$

with n=15, R=0.98, R^2=0.96, adj R^2=0.94, F(4,10)=54.17 (p<0.000001), outliers>2σ=0 and SD=0.06. Q_{10} is the net charge of atom 10 (see Fig. 2) and S_9^N is the total atomic nucleophilic superdelocalizability of atom 9. $F_2(HOMO-1)*$ is the Fukui index of the first highest local occupied MO of atom 2 and $F_{17}(LUMO)*$ is the Fukui index of the lowest local empty MO of atom 17. The beta coefficients and *t*-test for the significance of coefficients of Eq. 4 are shown in Table 4. Concerning independent variables, Table 5 shows that there are no

significant internal correlations. The associated statistical parameters of Eq. 4 show that this equation is statistically significant and that the variation of a group of local atomic reactivity indices belonging to the common skeleton explains about 94% of the variation of the cytotoxicity. Figure 4 shows the plot of observed values *vs.* calculated ones.

Table 4. Beta coefficients and t-test for the significance of coefficients in Eq. 4.

Variable	Beta	B	t(10)	p-level
S_9^N	**-0.64**	**-0.019201**	**-9.60**	**<0.000002**
$F_{17}(LUMO)*$	**0.69**	**0.741220**	**9.74**	**<0.000002**
Q_{10}	**0.40**	**3.273954**	**5.46**	**<0.0003**
$F_2(HOMO-1)*$	**-0.20**	**-0.541653**	**-2.84**	**<0.018**

Table 5. Squared correlation coefficients for the variables appearing in Eq. 4.

	S_9^N	$F_{17}(LUMO)*$	Q_{10}
$F_{17}(LUMO)*$	0.003	1.00	
Q_{10}	0.003	0.12	1.00
$F_2(HOMO-1)*$	0.01	0.0009	0.09

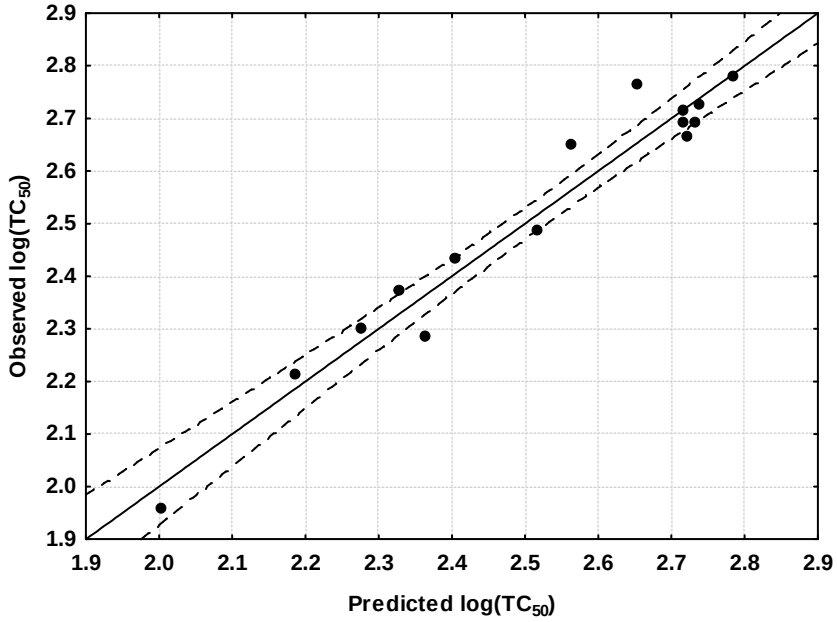

Figure 4. Plot of predicted *vs.* observed log(TC_{50}) values from Eq. 4. Dashed lines denote the 95% confidence interval.

DISCUSSION

Molecular electrostatic potential of the substituted acylamidobenzamides.

Figures 5-8 show, respectively, the MEP of molecules 2, 3, 7 and 8. Molecule 2 has the highest cytotoxicity and molecule 3 the lowest. Molecules 7 and 8 have, respectively, the lowest and highest anti-influenza activity (see Table 1).

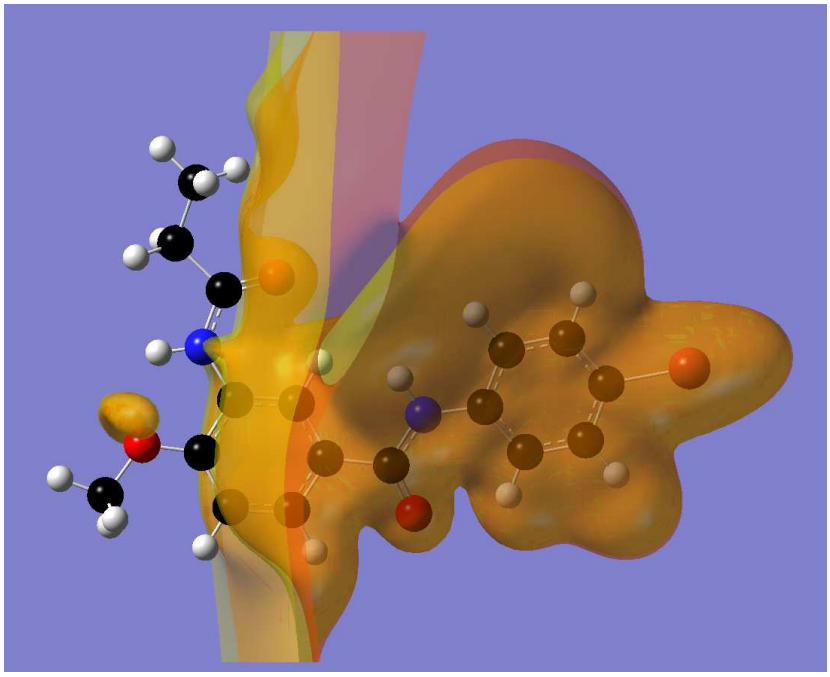

Figure 5. MEP of molecule 2. The orange isovalue surface corresponds to negative MEP values (-0.0004) and the yellow isovalue surface to positive MEP values (0.0004).

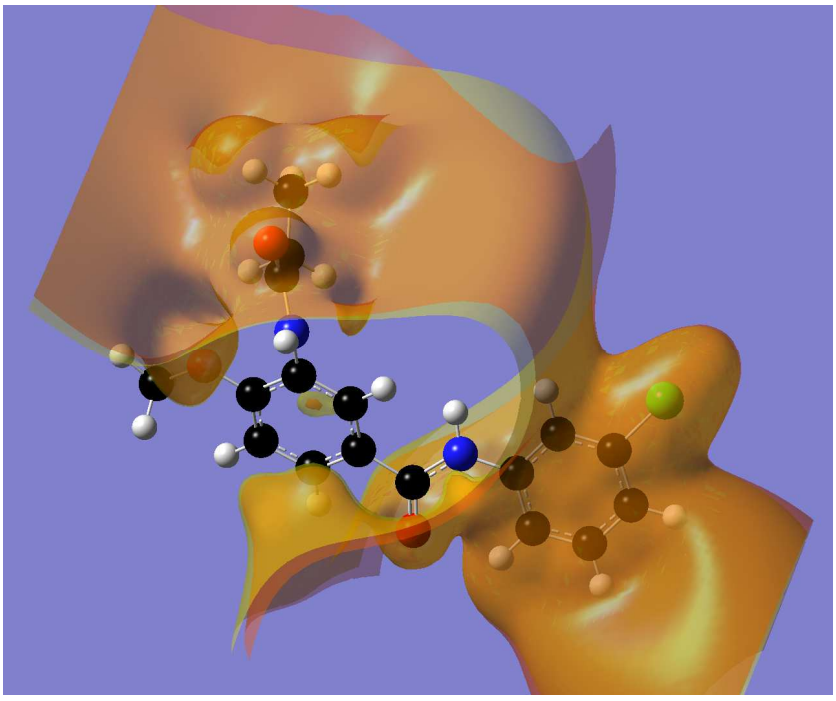

Figure 6. MEP of molecule 3. The orange isovalue surface corresponds to negative MEP values (-0.0004) and the yellow isovalue surface to positive MEP values (0.0004).

The comparison of Figs. 9 and 10 shows that a common area of negative MEP exists in the region of ring B (see Fig. 3). In the upper left side of both figures we can see that the three-dimensional structure of that negative MEP area is controlled by the relative position of the NH-C=O fragment of ring A. Considering that on one hand we are presenting the results for the lowest energy conformer and that on the other the NH-C=O fragment has enough conformational flexibility, we may conjecture that during all the process leading to the manifestation of cytotoxicity all molecules presenting this biological activity may adapt their MEP for any long-range recognition process [46]. We do not know if this process is a multi-step one or not. As the molecule's properties (i.e., the detailed electronic structure) that are responsible for the molecular interactions leading to the pharmacological effect are encoded in the whole molecular structure, even a molecule not displaying any biological activity could have a similar MEP structure.

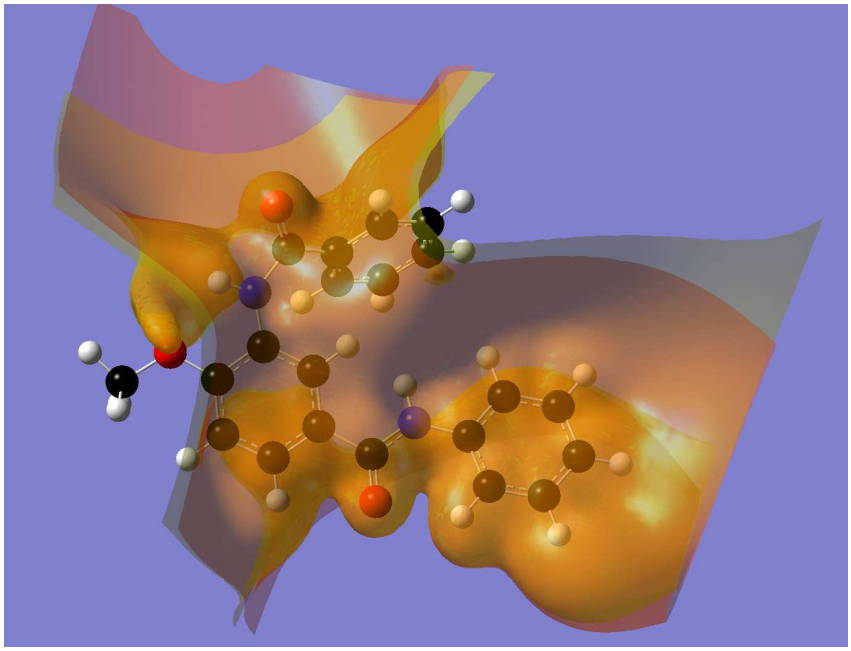

Figure 7. MEP of molecule 7. The orange isovalue surface corresponds to negative MEP values (-0.0004) and the yellow isovalue surface to positive MEP values (0.0004).

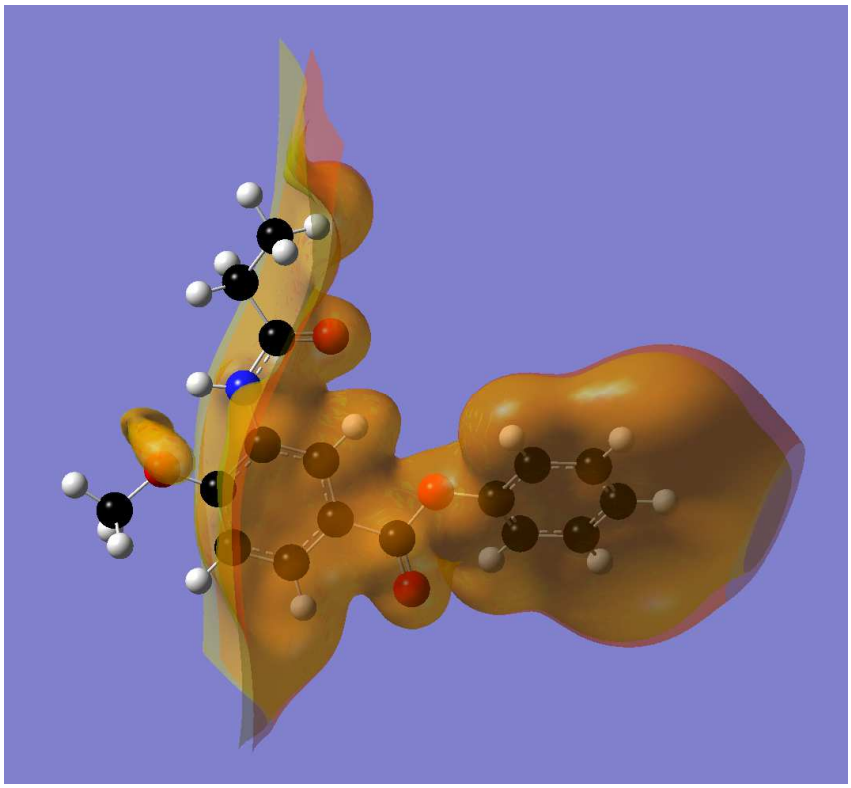

Figure 8. MEP of molecule 8. The orange isovalue surface corresponds to negative MEP values (-0.0004) and the yellow isovalue surface to positive MEP values (0.0004).

In molecule 8 the fragment C(O)-NH-Ring-B (see Fig. 7) was changed to C(O)-O-Ring-B (Fig. 8). We can appreciate that the three-dimensional (3D) structure of the region around ring B has not changed significantly. In the region of the upper left hand side of Figs. 7 and 8 the 3D structure of the MEP depends on the orientation of the NH-C=O fragment as in the previous case. As a general conclusion we may note that, due to the high conformational flexibility of these systems, we are not in a position to decide what the exact 3D MEP structure of these molecules is *during* their microscopic action. For small molecules, such as hallucinogenic amphetamines (acting as cations) or kynurenic acid derivatives (acting as zwitterions) this can be done with confidence [61, 76].

Frontier molecular orbitals of the substituted amidobenzamides.

Figures 9 and 10 show, respectively, the HOMO and LUMO of molecule 2.

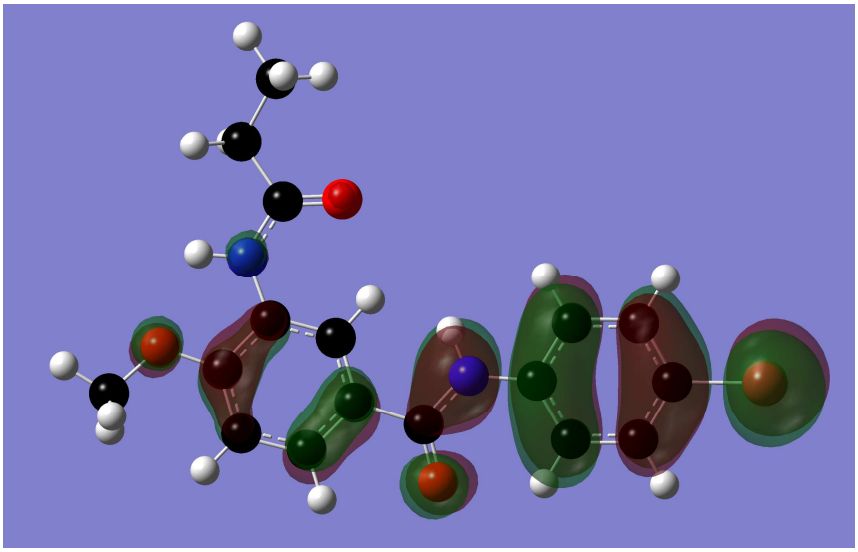

Figure 9. Localization of the highest occupied molecular orbital (HOMO) of molecule 2 (isovalue = 0.02).

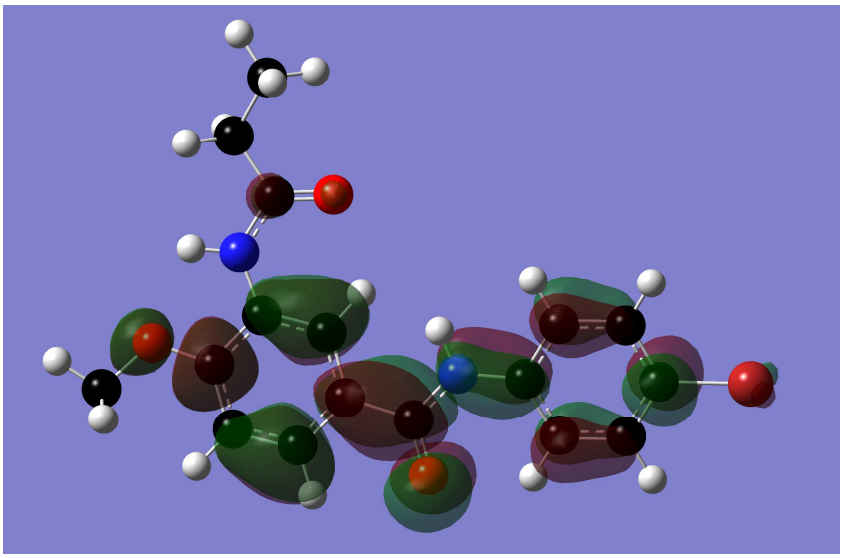

Figure 10. Localization of the lowest empty molecular orbital (LUMO) of molecule 2 (isovalue = 0.02).

In Fig. 9 we can see that the HOMO is localized on rings A and B, on the fragment joining them and on the bromine atom. This MO is of π nature. Note that the HOMO is not localized on atom 2 of the common skeleton (see Fig. 2). Then, if atom 2 donates charge it will do so, not from the molecular HOMO, but from the highest occupied molecular orbital localized on this atom (its local HOMO*). In fact, the local HOMO* of atom 2 corresponds to the second highest MO of the molecule (also of π nature, not shown here). The LUMO is localized on all atoms of rings A and B, the fragment joining them and the carbonyl groups, being of π nature (Fig. 10). Figure 11 shows the LUMO of molecule 20.

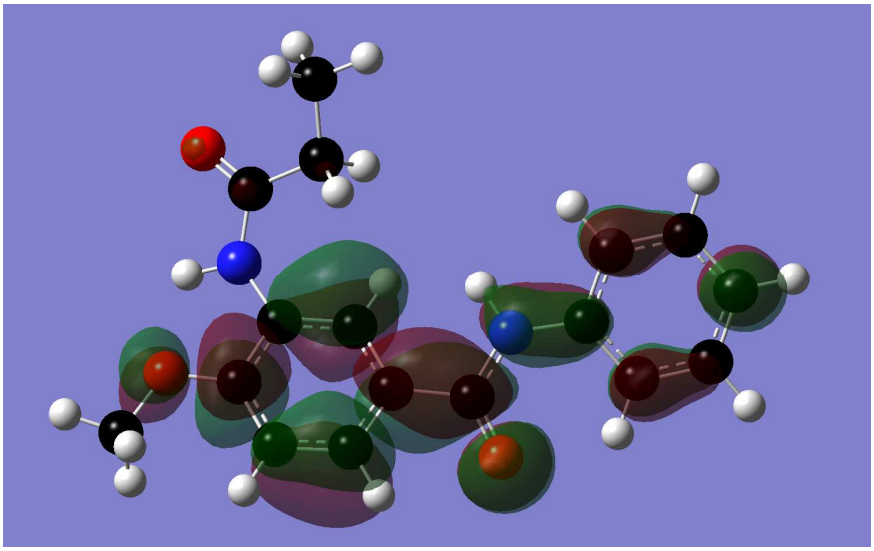

Figure 11. Localization of the LUMO of molecule 20 (isovalue = 0.02).

For this case we can see that the LUMO is not localized on atoms 15 and 17 of ring B. These differences between the LUMOs of molecules 2 and 20 are a good pictorial example of properties that could account for the differences in biological activities.

Analysis of the relationship between molecular structure and antiviral activity against the influenza A/Guangdong Luohu/219/2006 (H1N1) strain CPE of substituted amidobenzamides (Eq. 3).

There is a very important point that needs to be commented on before analyzing our results. In the previous analysis we have spoken of electron-donor areas, centers or moieties (and the same for electron-acceptor centers in other papers). In the following discussion we shall not include hydrogen bond formation by some heteroatoms belonging to an aromatic system because there are other local atomic reactivity indices describing them. Within the LCAO-MO framework a medium- or large-sized molecule possesses a group of occupied and vacant (empty) molecular orbitals. From a theoretical point of view the MOs can be classified as being of π, σ or n (lone pair) nature. In the usual quantum-chemical calculations we sometimes obtain MOs of a mixed nature: the MO has, for example, π nature in one molecular region and σ nature in another. Let us consider now what happens when an aromatic moiety interacts with a similar structure of a partner. This kind of interaction is called π-π stacking [77-79] (the face-centered π-π interaction between aromatic systems is not favored and will not be considered here). Regarding the interaction of aromatic systems, Sanders and Hunter pointed out that when we consider the interaction between two such π-systems, an attractive interaction is clearly counterintuitive because the dominant interaction will be the repulsion of the two most closely approaching π-clouds [79]. Also, the higher the local charge density on an atom in the highest MOs localized on it, the larger the size of the exclusion shell into which other electrons are not allowed to penetrate. Working with a very simple model these authors suggest that σ-π attraction dominates in an offset (off-centre) π-stacked geometry [79]. Here, and within our model of local atomic contributions and for the case of aromatic systems, we shall understand that the quasi-rigid σ framework charge of the i-th atom is constituted by the nuclear charge of the i-th atom minus the Fukui indices of the σ MOs localized on it. We can safely state that this atomic framework has a positive net charge and that *almost* all the σ MO eigenvalues are located below the eigenvalues of the π MOs. On the other hand, let us consider the total net charges of the atoms composing the aromatic system. It is also safe to state in a first approximation that for a particular orientation of two π-systems, positively charged atoms on one moiety tend to be aligned with negatively charged atoms on the other, so that there is an attractive electrostatic interaction. But this alignment will also be controlled by the repulsion of the π MOs: two atoms will tend to be aligned in such a way that the occupied π MOs localized on them minimize their repulsive interactions. The best ideal situation should be the interaction of a positively charged atom without occupied π MOs localized on it and with vacant π MOs localized on it, with a negatively charged atom with occupied π MOs localized on it. Last year, and within the LCAO-MO framework, we proposed a set of local atomic reactivity indices, several of which are employed in this paper [50]. In the light of the above discussion we think that two of them, the total local atomic density of occupied states and the total local atomic density of vacant (empty) states, may be useful to analyze the penetration of the electronic cloud into another molecular system. Therefore, when we interpret a local atomic partial reactivity index belonging to an aromatic system and appearing in a equation (a partial reactivity index is one depending on only one MO), we are most probably only getting a partial picture of what is happening there.

The Beta values (Table 3) indicate that the importance of the variables is $s_{17} > S_7^E(HOMO-2)^* > F_4(LUMO+2)^* > F_{16}(LUMO+2)^* = S_{11}^E(HOMO-1)^*$. Almost all points in Fig. 3 are within the 95% confidence interval suggesting that the common skeleton employed for this case is reliable. A variable-by-variable analysis of Eq. 3 indicates that good antiviral activity is associated with high values for s_{17} and $S_{11}^E(HOMO-1)^*$ and with low values for $S_7^E(HOMO-2)^*$, $F_4(LUMO+2)^*$ and $F_{16}(LUMO+2)^*$. A high value for s_{17} indicates that the local HOMO*-LUMO* gap should be small. If we identify the local atomic softness with the local atomic charge capacity defined as the ability to retain electronic charge once it has been acquired [50], we suggest that atom 17 should act as a strong electron-acceptor center and should be prone to modify its electronic density quite easily. A high value for $S_{11}^E(HOMO-1)^*$ indicates that atom 11 acts as an electron-donor center in a π-π stacking interaction. Knowing that $S_{11}^E(HOMO)^*$ has a non-zero value it is clear that at least the two highest occupied local MOs of atom 11 participate in the interaction. The nonappearance of $S_{11}^E(HOMO)^*$ in Eq. 3 is due to the fact that the variation of this reactivity index through the series is not statistically significant (i.e., its value is too small and/or constant). A low value for $S_7^E(HOMO-2)^*$ can be interpreted as follows. As an example, let us analyze the case of molecule 2. For this molecule the local $(HOMO-2)_7^*$ is the fourth highest occupied molecular MO. Figure 12 shows the structure and localization of the fourth highest occupied molecular orbital (HOMO-3) of molecule 2.

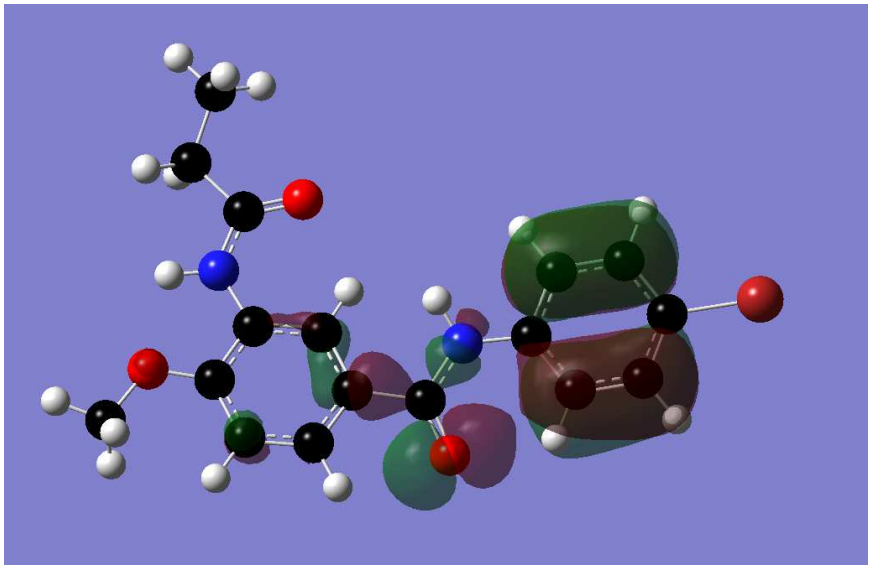

Figure 12. Localization of the fourth highest occupied molecular orbital (HOMO-3) of molecule 2 (isovalue = 0.02).

This MO is of π nature on ring B and of nature in the fragment joining both aromatic rings. In comparison with π MOs, the σ electronic density can be considered as being quasi-non-deformable. If atom 7 is acting as an electron-acceptor center, then the low or zero localization of $(HOMO2)_7^*$ on it will facilitate the interaction by diminishing the repulsive electron-electron interaction between the occupied MOs of both partners (let us remember that the larger the charge density on an atom, the larger the size of the exclusion volume into which other electrons are not allowed to penetrate). It is interesting to note that in the original formulation of Klopman and Hudson (Refs. [80-82]) three terms appeared in their final equations: the interaction of net charges belonging to both partners and the attractive interactions of the occupied (empty) MOs of one partner with the empty (occupied) MOs of the other. But, within this scheme, it is natural to consider that there are also repulsive interactions between the occupied MOs of one partner with the occupied MOs of the other. A theoretical treatment of these repulsive interactions within the LCAO-MO framework and the model presented in Ref. [50] has yet to be done. These repulsive interactions may occur between any combination of π, σ and n MOs. The analysis of each particular case is mandatory for suggesting hypothetical action mechanisms. The cases of $F_4(LUMO+2)^*$ and $F_{16}(LUMO+2)^*$ can be interpreted as follows. Let us consider again molecule 2. For atom 4, $LUMO_4^*$ is the molecule's LUMO, $(LUMO+1)_4$ is the fourth highest empty molecular MO and $(LUMO+2)_4$ is the sixth highest empty molecular MO. In the case of atom 16, $LUMO_{16}^*$ is the molecular LUMO, $(LUMO+1)_{16}^*$ is the third highest empty molecular MO and $(LUMO+2)_{16}^*$ is the fourth highest empty molecular MO. All these MOs are of π nature. With all these considerations we can speculate that a low localization of (LUMO+2)* on atoms 4 and 16 may facilitate the interaction of their corresponding (LUMO+1)* and LUMO* MOs in a π-π stacking interaction with another aromatic moiety. The two-

dimensional (2D) antiviral pharmacophore, containing all the above suggestions, is shown in Fig. 13. It must be stressed that this antiviral pharmacophore only contains those properties whose variation gives an account of the variation of the antiviral activity in the series of molecules. In this sense this pharmacophore can be considered as a partial construct.

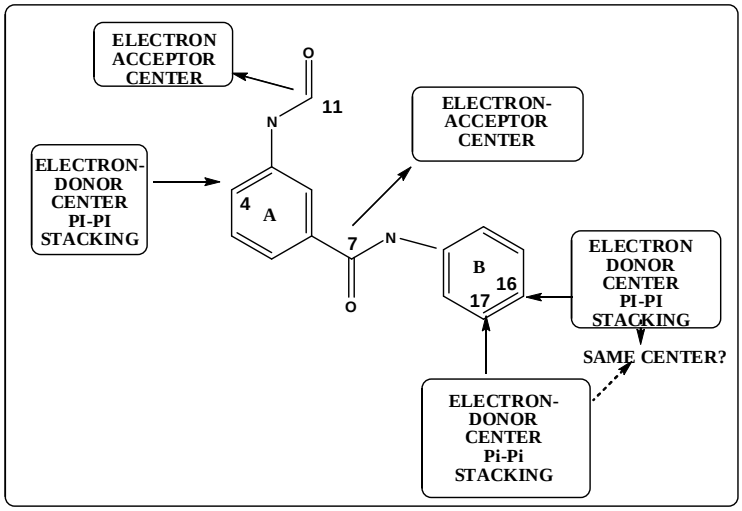

Figure 13. Partial 2D antiviral pharmacophore for substituted amidobenzamides.

Analysis of the relationship between molecular structure and cytotoxicity of substituted amidobenzamides in MDCK cells (Eq. 4).

The beta values (Table 4) indicate that the importance of the variables is $F_{17}(LUMO)^* = S_9^N > Q_{10} > F_2(HOMO-1)^*$. Almost all points in Fig. 6 are within the 95% confidence interval suggesting that the common skeleton employed for cytotoxicity analysis is trustworthy. A variable-by-variable analysis of Eq. 4 indicates that high cytotoxicity is associated with high values for S_9^N and $F_2(HOMO-1)^*$, with a negative net charge on atom 10 and with a low value for $F_{17}(LUMO)^*$. The sign of the net charge on atom 10 (nitrogen) will be regulated by the nature of the substituents attached to the C_{11}-O_{12} fragment and by the substituents on ring A (Fig. 3). Atom 10 might participate in the process leading to cytotoxicity through an electrostatic interaction with a positive region (helped by the negative net charge of O_{12}) or through a hydrogen bond (with OH, NH or SH groups). A high value for S_9^N suggests that atom 9 participates as an electron-acceptor center. The appearance of $F_2(HOMO-1)^*$ indicates that atom 2 participates as an electron-donor center including its $HOMO_2$* in a π-π stacking interaction. A low value for $F_{17}(LUMO)^*$, which is of π nature in all the molecules studied here, can be rationalized by suggesting that atom 17 acts as an electron-donor center in a π-π stacking interaction. A high value for $F_{17}(LUMO)^*$ could interfere, through repulsive empty MO-empty MO interactions, with an optimal interaction of atom 17 with a partner. All these suggestions are summarized in Fig. 14.

Despite the fact that the action mechanisms for both antiviral and cytotoxic activities are not known for the compounds studied here, statistically significant equations have been obtained for both of them. The equations explain the variation of these activities throughout a family of molecules in terms of the variation of the numerical values of different sets of local atomic reactivity indices belonging to the proposed common skeleton. Unhappily, our lack of knowledge about the microscopic action mechanism does not allow us to assign the terms appearing in Eq. 3 and 4 to any particular process. Regarding the accuracy of the common skeleton, whose structure was chosen before the calculations, the good results obtained validate the actual choice. This does not always happen [54]. The information obtained from this study, and depicted in the corresponding 2D partial pharmacophores, should be useful for researchers devoted to the synthesis and testing of this kind of compounds.

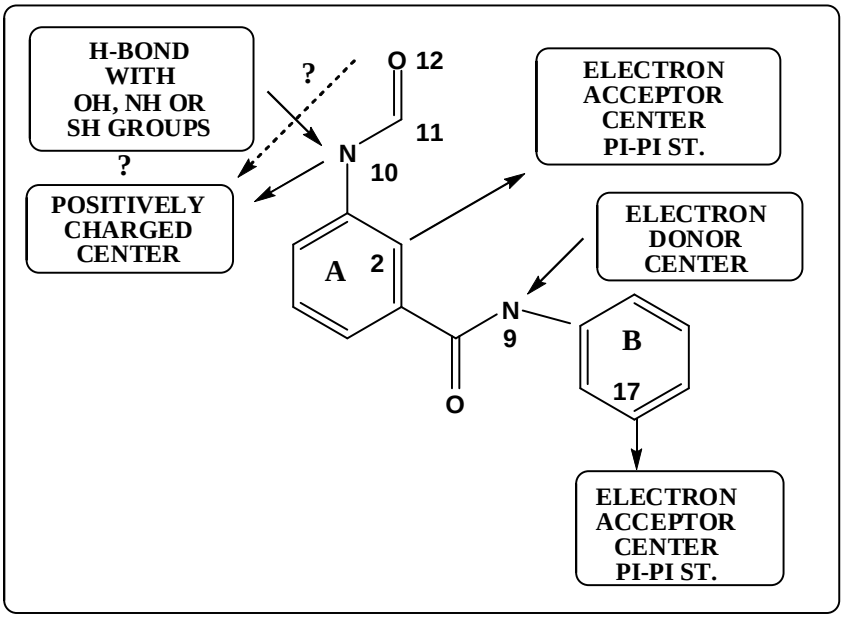

Figure 14. Partial 2D cytotoxicity pharmacophore for substituted amidobenzamides.

The ideal situation for studies like the one presented here, a situation that is very hard to find in the specialized literature, is to have very long lists of molecules with multiple substitutions at multiple sites with the corresponding biological activities measured in (almost) identical experimental settings. This will guarantee that these reported values are comparable and that they can be used to form a single set. It is also important to stress the success of this method despite the large number of approximations used. The local atomic reactivity indices here are the product of several physically-based simplifications. Moreover, their numerical values are obtained from an *in vacuo* full geometry optimization of the molecule. This fact implies at least two hypotheses: that this geometry is very close to the biologically active conformation and that these molecules act after losing any solvent molecule (water, ions) that they were interacting with. On the other hand, the action mechanism(s) of these substituted amidobenzamides involves non-covalent interactions. Then, a description of the whole system in terms of its isolated constituent parts (unperturbed drug and partner(s)) is suitable and seems to be very useful for the identification of molecular structural factors affecting biological activity. Keeping the Orientational Factors and the electrostatic interaction of the net charges of both partners aside, the MO-MO interactions between them can be classified into three types. The first is the charge transfer between occupied MOs of the drug and the vacant MOs of the partner and vice versa. The second is the interaction between occupied MOs of the drug and occupied MOs of the partner (causing electron exchange and delocalization between molecules) and the interaction of vacant MOs of the drug with the occupied MOs of the partner. The last one is the classical electrostatic interaction between occupied MOs of both partners. It seems that our local atomic reactivity indices can explain, if not all, almost all these interactions.

In conclusion, despite the almost total lack of knowledge regarding the mechanisms of antiviral action and cytotoxicity in these cases, we have obtained statistically significant relationships between electronic structure and antiviral and cytotoxic activities. The variation of the antiviral activity is mainly orbital-controlled [82]. The variation of cytotoxicity is charge- and orbital-controlled. The common skeleton used for this study seems to be correct.

REFERENCES

[1]Y Guan; D Vijaykrishna; J Bahl; H Zhu; J Wang; GD Smith, *Prot. Cell*, **2010**, 1, 9-13.
[2]M Zambon, *Medicine*, **2014**, 42, 45-51.
[3]DM Morens; JK Taubenberger; AS Fauci, *New Eng. J. Med.*, **2013**, 368, 2345-2348.
[4]SJ Gamblin; LF Haire; RJ Russell; DJ Stevens; B Xiao; Y Ha; N Vasisht; DA Steinhauer; RS Daniels; A Elliot; DC Wiley; JJ Skehel, *Science*, **2004**, 303, 1838-1842.
[5]W Zheng; YJ Tao, *FEBS Letters*, **2013**, 587, 1206-1214.
[6]A Vincent; L Awada; I Brown; H Chen; F Claes; G Dauphin; R Donis; M Culhane; K Hamilton; N Lewis; E Mumford; T Nguyen; S Parchariyanon; J Pasick; G Pavade; A Pereda; M Peiris; T Saito; S Swenson; K Van Reeth; R Webby; F Wong; J Ciacci-Zanella, *Zoon. Pub. Health*, **2013**, n/a-n/a.

[7]Q Teng; X Zhang; D Xu; J Zhou; X Dai; Z Chen; Z Li, *Vet. Microbiol.*, **2013**, 162, 345-352.
[8]Y Sun; S Sun; J Ma; Y Tan; L Du; Y Shen; Q Mu; J Pu; D Lin; J Liu, *Virol.*, **2013**, 435, 301-307.
[9]X Sun; X Xu; Q Liu; D Liang; C Li; Q He; J Jiang; Y Cui; J Li; L Zheng; J Guo; Y Xiong; J Yan, *Inf. Gen. Evol.*, **2013**, 20, 471-475.
[10]S Su; H-T Li; F-R Zhao; J-D Chen; J-x Xie; Z-M Chen; Z Huang; Y-M Hu; M-Z Zhang; L-K Tan; G-H Zhang; S-J Li, *Inf. Gen. Evol.*, **2013**, 14, 444-449.
[11]Q-q Song; F-x Zhang; J-j Liu; Z-s Ling; Y-l Zhu; S-j Jiang; Z-j Xie, *Vet. Microbiol.*, **2013**, 161, 331-333.
[12]M Imai; S Herfst; EM Sorrell; EJA Schrauwen; M Linster; M De Graaf; RAM Fouchier; Y Kawaoka, *Vir. Res.*, **2013**, 178, 15-20.
[13]Y Cong; B-k Li; X-g Yang; Y Xue; Y-z Chen; Y Zeng, *Chemo. Int. Lab. Systems*, **2013**, 127, 35-42.
[14]X Xi; Q Fang; Q Gu; B Du, *J. Crit. Care*, **2013**, 28, 528-530.
[15]H-S Wu; J-H Chuang; F-Y Chang, *J. Formos. Med. Ass.*, **2013**, 112, 299-301.
[16]R-B Tang; H-L Chen, *J. Chin. Med. Ass.*, **2013**, 76, 245-248.
[17]JC Jones; T Baranovich; BM Marathe; AF Danner; JP Seiler; J Franks; EA Govorkova; S Krauss; RG Webster, *J. Virol.*, **2014**, 88, 1175-1188.
[18]M Stincarelli; R Arvia; MA De Marco; V Clausi; F Corcioli; C Cotti; M Delogu; I Donatelli; A Azzi; S Giannecchini, *Vir. Res.*, **2013**, 175, 151-154.
[19]R Zu; L Dong; X Qi; D Wang; S Zou; T Bai; M Li; X Li; X Zhao; C Xu; X Huo; N Xiang; S Yang; Z Li; Z Xu; H Wang; Y Shu, *Virol.*, **2013**, 446, 49-55.
[20]V Gregory; W Lim; K Cameron; M Bennett; S Marozin; A Klimov; H Hall; N Cox; A Hay; YP Lin, *J. Gen. Virol.*, **2001**, 82, 1397-1406.
[21]S Shikha Srivastava; N Misra; U Misra, *Der Pharm. Lett.*, **2009**, 1, 1-20.
[22]P Yang; Q Wang; X Pang; L Chen; L Tian; Y Deng, *J. Infect.*, **2013**, 67, 624-625.
[23]V Wiwanitkit, *J. Chin. Med. Ass.*, **2013**, 76, 532.
[24]M Ozawa; Y Kawaoka, *Ann. Rev. Anim. Biosci.*, **2013**, 1, 21-42.
[25]X-S Zhang; D De Angelis; PJ White; A Charlett; RG Pebody; J McCauley, *Epidemics*, **2013**, 5, 20-33.
[26]W-J Shin; BL Seong, *Exp. Op. Drug Discov.*, **2013**, 8, 411-426.
[27]L Menéndez-Arias; F Gago, "Antiviral Agents: Structural Basis of Action and Rational Design," in *Structure and Physics of Viruses*, M. G. Mateu Ed., vol. 68, pp. 599-630, Springer Netherlands, 2013.
[28]L Cegolon; C Salata; E Piccoli; V Juarez; G Palu'; G Mastrangelo; A Calistri, *Int. J. Hyg. Envir. Health*, **2014**, 217, 17-22.
[29]X Xiong; A Tuzikov; PJ Coombs; SR Martin; PA Walker; SJ Gamblin; N Bovin; JJ Skehel, *Vir. Res.*, **2013**, 178, 12-14.
[30]SP Singh; D Gogoi; RL Bezbaruah; MJ Bordoloi; NC Barua, *Drug Inv. Tod.*, **2013**, 5, 241-245.
[31]L Martinez-Gil; JG Alamares-Sapuay; MV Ramana Reddy; PH Goff; E Premkumar Reddy; P Palese, *Antiv. Res.*, **2013**, 100, 29-37.
[32]E Krol; I Wandzik; B Gromadzka; D Nidzworski; M Rychlowska; M Matlacz; J Tyborowska; B Szewczyk, *Antiv. Res.*, **2013**, 100, 90-97.
[33]U Kessler; D Castagnolo; M Pagano; D Deodato; M Bernardini; B Pilger; C Ranadheera; M Botta, *Bioorg. Med. Chem. Lett.*, **2013**, 23, 5575-5577.
[34]AV Ivachtchenko; YA Ivanenkov; OD Mitkin; PM Yamanushkin; VV Bichko; IA Leneva; OV Borisova, *Antiv. Res.*, **2013**, 100, 698-708.
[35]H Cheng; J Wan; M-I Lin; Y Liu; X Lu; J Liu; Y Xu; J Chen; Z Tu; Y-SE Cheng; K Ding, *J. Med. Chem.*, **2012**, 55, 2144-2153.
[36]M Mousavi; M Monajjemi; R Rasoolzadeh; A Karimi, *Clin. Biochem.*, **2011**, 44, S105.
[37]BK Mai; MS Li, *Biochem. Biophys. Res. Comm.*, **2011**, 410, 688-691.
[38]S Liu; R Li; R Zhang; CCS Chan; B Xi; Z Zhu; J Yang; VKM Poon; J Zhou; M Chen; J Münch; F Kirchhoff; S Pleschka; T Haarmann; U Dietrich; C Pan; L Du; S Jiang; B Zheng, *Eur. J. Pharmacol.*, **2011**, 660, 460-467.
[39]Y Kumaki; CW Day; DF Smee; JD Morrey; DL Barnard, *Antiv. Res.*, **2011**, 92, 329-340.
[40]E Khurana; RH DeVane; M Dal Peraro; ML Klein, *Biochem. Biophys. Scta - Biomemb.*, **2011**, 1808, 530-537.
[41]L Gao; M Zu; S Wu; A-L Liu; G-H Du, *Bioorg. Med. Chem. Lett.*, **2011**, 21, 5964-5970.
[42]V Tripathi; S Sankrit; DK Gupta, *Arch. App. Sci. Res.*, **2010**, 2, 93-97.
[43]KK Tapara; RD Jawarkar; VV Paithankar; PN Khataleb; AN Manikraob; BE Bhumesh E.Wanjaric; T Ben-Hadda, *J. Comput. Method. Mol. Design*, **2011**, 1, 1-6.
[44]YC Martin, *Quantitative drug design: a critical introduction*, M. Dekker, New York, 1978.
[45]JS Gómez-Jeria, *Int. J. Quant. Chem.*, **1983**, 23, 1969-1972.
[46]JS Gómez-Jeria, "Modeling the Drug-Receptor Interaction in Quantum Pharmacology," in *Molecules in Physics, Chemistry, and Biology*, J. Maruani Ed., vol. 4, pp. 215-231, Springer Netherlands, 1989.
[47]T Bruna-Larenas; JS Gómez-Jeria, *Int. J. Med. Chem.*, **2012**, 2012 Article ID 682495, 1-16.
[48]DA Alarcón; F Gatica-Díaz; JS Gómez-Jeria, *J. Chil. Chem. Soc.*, **2013**, 58, 1651-1659.

[49]JS Gómez-Jeria, *Elements of Molecular Electronic Pharmacology (in Spanish)*, Ediciones Sokar, Santiago de Chile, 2013.
[50]JS Gómez-Jeria, *Canad. Chem. Trans.*, **2013**, 1, 25-55.
[51]I Reyes-Díaz; JS Gómez-Jeria, *J. Comput. Methods Drug Des.*, **2013**, 3, 11-21.
[52]JS Gómez-Jeria, *Int. Res. J. Pure App. Chem.*, **2014**, 4, 270-291.
[53]JS Gómez-Jeria, *Der Pharmacia Lettre*, **2014**, in press.,
[54]F Salgado-Valdés; JS Gómez-Jeria, *J. Quant. Chem.*, **2014**, 2014 Article ID 431432, 1-15.
[55]K Fukui; H Fujimoto, *Frontier orbitals and reaction paths: selected papers of Kenichi Fukui*, World Scientific, Singapore; River Edge, N.J., 1997.
[56]JS Gómez-Jeria; M Ojeda-Vergara; C Donoso-Espinoza, *Mol. Engn.*, **1995**, 5, 391-401.
[57]JS Gómez-Jeria; M Ojeda-Vergara, *J. Chil. Chem. Soc.*, **2003**, 48, 119-124.
[58]JS Gómez-Jeria; D Morales-Lagos, "The mode of binding of phenylalkylamines to the Serotonergic Receptor," in *QSAR in design of Bioactive Drugs*, M. Kuchar Ed., pp. 145-173, Prous, J.R., Barcelona, Spain, 1984.
[59]JS Gómez-Jeria; DR Morales-Lagos, *J. Pharm. Sci.*, **1984**, 73, 1725-1728.
[60]JS Gómez-Jeria; P Sotomayor, *J. Mol. Struct. (Theochem)*, **1988**, 166, 493-498.
[61]JS Gómez-Jeria; L Lagos-Arancibia, *Int. J. Quant. Chem.*, **1999**, 71, 505-511.
[62]JS Gómez-Jeria; L Lagos-Arancibia; E Sobarzo-Sánchez, *Bol. Soc. Chil. Quím.*, **2003**, 48, 61-66.
[63]JS Gómez-Jeria; F Soto-Morales; G Larenas-Gutierrez, *Ir. Int. J. Sci.*, **2003**, 4, 151-164.
[64]JS Gómez-Jeria; LA Gerli-Candia; SM Hurtado, *J. Chil. Chem. Soc.*, **2004**, 49, 307-312.
[65]JS Gómez-Jeria; F Soto-Morales; J Rivas; A Sotomayor, *J. Chil. Chem. Soc.*, **2008**, 53, 1393-1399.
[66]JS Gómez-Jeria, *J. Chil. Chem. Soc.*, **2010**, 55, 381-384.
[67]JS Gómez-Jeria; D Morales-Lagos; JI Rodriguez-Gatica; JC Saavedra-Aguilar, *Int. J. Quant. Chem.*, **1985**, 28, 421-428.
[68]JS Gómez-Jeria; D Morales-Lagos; BK Cassels; JC Saavedra-Aguilar, *Quant. Struct.-Relat.*, **1986**, 5, 153-157.
[69]JS Gómez-Jeria; BK Cassels; JC Saavedra-Aguilar, *Eur. J. Med. Chem.*, **1987**, 22, 433-437.
[70]JS Gómez-Jeria; M Flores-Catalán, *Canad. Chem. Trans.*, **2013**, 1, 215-237.
[71]C Barahona-Urbina; S Nuñez-Gonzalez; JS Gómez-Jeria, *J. Chil. Chem. Soc.*, **2012**, 57, 1497-1503.
[72]A Paz de la Vega; DA Alarcón; JS Gómez-Jeria, *J. Chil. Chem. Soc.*, **2013**, 58, 1842-1851.
[73]MJ Frisch; GW Trucks; HB Schlegel; et al., Gaussian98 Rev. A.11.3, Gaussian, Pittsburgh, PA, USA, 2002.
[74]JS Gómez-Jeria, *J. Chil. Chem. Soc.*, **2009**, 54, 482-485.
[75]Statsoft, Statistica 8.0, 2300 East 14 th St. Tulsa, OK 74104, USA, 1984-2007.
[76]JS Gómez-Jeria, *Acta sud Amer. Quím.*, **1984**, 4, 1-9.
[77]CR Martinez; BL Iverson, *Chem. Sci.*, **2012**, 3, 2191-2201.
[78]SL Cockroft; CA Hunter; KR Lawson; J Perkins; CJ Urch, *J. Am. Chem. Soc.*, **2005**, 127, 8594-8595.
[79]CA Hunter; JKM Sanders, *J. Am. Chem. Soc.*, **1990**, 112, 5525-5534.
[80]RF Hudson; G Klopman, *Tet. Lett.*, **1967**, 8, 1103-1108.
[81]G Klopman; RF Hudson, *Theoret. Chim. Acta*, **1967**, 8, 165-174.
[82]G Klopman, *J. Am. Chem. Soc.*, **1968**, 90, 223-234.